Carbohydrate Polymers 94 (2013) 829–835

Contents lists available at SciVerse ScienceDirect

Carbohydrate Polymers

journal homepage: www.elsevier.com/locate/carbpol

Polysaccharide of *Hohenbuehelia serotina* as a defense against damage by whole-body gamma irradiation of mice

Xiaoyu Li[a], Zhenyu Wang[a,b,*], Lu Wang[a]

[a] Harbin Institute of Technology, 73 Huanghe Road, Nangang District, Harbin 150090, PR China
[b] Northeast Forestry University, 26 Hexing Road, Xiangfang District, Harbin 150040, PR China

ARTICLE INFO

Article history:
Received 27 November 2012
Received in revised form 19 January 2013
Accepted 11 February 2013
Available online 18 February 2013

Keywords:
Hohenbuehelia serotina
Polysaccharide
Antioxidant activity
Immunomodulation activity
Radioprotective effect

ABSTRACT

This study was designed to investigate the antioxidant, immunomodulation and radioprotective activities of the polysaccharides from *Hohenbuehelia serotina* (HSP) against the damages induced by ^{60}Co-radiation in vivo. Antioxidant results showed that the mice treated with HSP could effectively increase the superoxide dismutase (SOD) and catalase (CAT) activities, and reduce the malondialdehyde (MDA) level after 6 Gy irradiation compared to irradiated, non-treated controls. Administration with HSP (200 mg/kg BW) significantly promote the proliferation of splenocytes ($p < 0.01$), and prevent the number of the blood WBC decrease and the function of hematopoietic decline which caused by irradiation in whole blood. HSP displayed strong immunomodulation activity in vivo, and the effect was further verified by the assay of monocyte phagocytosis. In addition, HSP significantly inhibit irradiation-induced spleen cells arrest into G0/G1 phase. These results suggested that HSP exerts an effective protection against radiation-induced injury by improving the antioxidant and immunomodulation activities.

1. Introduction

Nowadays, radiation is the important treatment of choice for most of cancer patients. However, exposure to radiation can produce severe health impairments for long time, especially the surrounding normal tissues (Park, Hwang, Song, & Jee, 2011). In the therapy of radiation process, a majority of free radicals were produced which could trigger the oxidative reactions of biological macromolecules, including proteins, lipids and polysaccharides. These oxidation products further modified and attacked DNA, proteins and lipids nearby, causing cellular chain damage (Thotala et al., 2009). Radioprotectors are essential in safeguarding the normal tissue during intended radiation exposure. At present, the most effective radioprotectors are thiol compounds; however, they have high toxicity that could produce toxic side effects on the body for taking a long time (Yu, Piao, Pei, Qi, & Hua, 2010). Natural products served as new type of radioprotector possess a good effect and low toxicity characteristics which offset the shortcomings of thiol compounds (Lata et al., 2009). Various natural radioprotective products have been discovered, including polyphenol, anthocyanins (Bansal et al., 2012) and especially polysaccharide (Zhao et al., 2012). Polysaccharides from edible mushroom have been conformed to have lots of biological activities, such as antioxidant (Cheng, Feng, Jia, Li, Zhou, & Ding, 2013; Wang, Mao, & Wei, 2012), anti-tumor (Sun et al., 2013; Yang, Pei, Shi, Zhao, Fang, & Hu, 2012), immunomodulation (Patra et al., 2013; Wang, Wang, Liu, Yuan, & Yue, 2013), therefore, attracted much attention in the fields of biochemistry and pharmacology.

In recent years, there has been a growing trend in the consumption of mushrooms and their products, including the *Hohenbuehelia serotina*, *Lentinus edodes* and *Auricularia Auricula*. *H. serotina*, described as "anmo" is a key member of the Chinese mushrooms which is famous for its antioxidant and anti-tumor effects. It is well-accepted by consumers in China and other Asian countries. *H. serotina* belongs to Pleurotaceae, and is widely distributed in the areas of the North Hemisphere, especially in the Northeast of China. We have reported the primary structure of the polysaccharide from *H. serotina*. The objective of this study was to investigate the anti-radiation effect of the polysaccharides from the fruiting body of *H. serotina* in vivo.

2. Materials and methods

2.1. Materials and reagents

The dried *H. serotina* mushroom was purchased from a local commercial market and the producing area was Shangzhi, Heilongjiang Province, China. The voucher specimen was identified

* Corresponding author at: School of Food Science and Engineering, Harbin Institute of Technology, 73 Huanghe Road, Nangang District, Harbin 150090, PR China. Tel.: +86 045186282909; fax: +86 045186282909.
E-mail addresses: smallrainlee@gmail.com, wzy219001@yahoo.com.cn (Z. Wang).

0144-8617/$ – see front matter © 2013 Elsevier Ltd. All rights reserved.
http://dx.doi.org/10.1016/j.carbpol.2013.02.015

by Zhenyu Wang, College of Food Science and Engineering, Harbin Institute of Technology, China. Distillation phenol was purchased from Sigma Chemical Co (St. Louis, MO, USA). Fatal bovine serum (FBS), L-glutamine, penicillin, and streptomycin were bought from Life Technologies, Inc. (Gaithersburg, MD). All chemicals were of analytical grade purchased from local suppliers.

2.2. Preparation of crude polysaccharides

Fruiting bodies of *H. serotina* were smashed and passed through 200 mesh sieve. All the mushroom powders were defatted with petroleum ether overnight. The polysaccharides present in *H. serotina* were extracted following the method reported by Ying, Han, and Li (2011) with a few modifications (Ying et al., 2011). Briefly, the ground powder was extracted with one hundred volumes of distilled water at 90 °C for ultrasound treatment 20 min and incubated for 3 h in a water-bath set at 90 °C. The processes were carried out in triplicate. The extracts were then combined and separated by filtration on a Buchner funnel and centrifuged using centrifuge at 8000 rpm for 10 min. The supernatant was collected and concentrated with a rotary evaporator at 50 °C under vacuum. Then, extracts were precipitated with three volumes of 95% ethanol overnight. All the pellets were washed with absolute ethanol, acetone and ether independently, then re-dissolved into a small amount of distilled water and lyophilized. The total carbohydrates of HSP were determined by the phenol-sulfuric acid method with D-glucose as standard (Zou, Chen, Yang, & Liu, 2011). The polysaccharides were stored in −20 °C for further analysis.

2.3. Primary structure analysis of HSP

2.3.1. Determination of molecular weight-HPGPC

The molecular weight of HSP was determined by gel permeation chromatography (HPGPC), which was performed on an Agilent 1100 series system fitted with one TSK = G5000PW$_{XL}$ (7 μm, 30 mm × 7.8 mm i.d.) column and an Agilent 1100 series refractive index (RI) detector. The sample was diluted to a concentration of 2 mg/mL and centrifuged at 12,000 rpm for 10 min, and then passed through 0.45 μm filter. 20 μL of the supernatant was injected in each run. The column and RI detector temperatures were constantly kept at 30 °C. The 0.2 M Na_2SO_4 solution was pumped to an HPLC system at the flow rate of 0.8 mL/min at 35 °C. The molecular mass was reported relative to Dextran standards, and was measured according to the method by Hsu, Hsu, Lin, Cheng, and Yang (2013).

2.3.2. Monosaccharide component analysis

The monosaccharide analysis was performed by gas chromatography (GC) method as described by Liu, Sun, Yu, and Liu (2012) with some slight modifications. Briefly, HSP (2 mg) was dissolved in 4 mL of 2 mol/mL trifluoroacetic acid solution (TFA) and hydrolyzed at 110 °C for 4 h. After removing the residual TFA with methanol under reduced pressure, the sample was dissolved in 1.0 mL of pyridine and reacted with 10 mg of hydroxylamine hydrochloride and 2 mg of inositol for 30 min at 90 °C. Afterwards, 3 mL of acetic anhydride was added and incubated for another 3 h at 90 °C. Seven standard sugars (rhamnose, arabinose, xylose, mannose, glucose, ribose and galactose) were converted to their acetylated derivatives according to the above-mentioned method.

2.3.3. IR spectroscopy

The IR spectrum of HSP was determined using a Fourier transform infrared spectrophotometer. The sample was ground with spectroscopic grade potassium bromide (KBr) powder and then pressed into 1 mm pellets for FT-IR determination in the frequency range of 4000–400 cm^{-1}.

2.4. Animals

Male KM mice of SPF-level (6–8 weeks old, weighing 18–22 g each) were obtained from the Laboratory Animal Center of Harbin Medical University and were housed under specific pathogen-free conditions. The animal room was controlled for temperature (22 ± 2 °C), light (12 h light/dark cycles) and humidity (50% ± 10%). Rodent laboratory chow pellets and tap water were randomly supplied. The experimental protocol was approved by Institutional Animal Ethical committee.

2.5. Experimental design and oral administration

This experiment was conducted as follows:
Group I: Radiation + HSP (50 mg/kg BW/D)
Group II: Radiation + HSP (100 mg/kg BW/D)
Group III: Radiation + HSP (200 mg/kg BW/D)
Group IV: Radiation + Leucogen (12 mg/kg BW/D) (Positive control group)
Group V: Radiation (Model group)
Group VI: Normal mice (Normal group)

60 healthy male mice were randomly divided into six groups. One group was served as normal control. The polysaccharides were administered using vehicle solution (deionized water). The animal in Normal and Model groups serving as normal control and radiation control were orally received deionized water only.

Groups I–III were administered with HSP at the dose of 50 mg/kg, 100 mg/kg and 200 mg/kg BW/D in the same solvent. After two weeks of treatment, the animals were received the full bodies radiation of ^{60}Co (6 Gy). Then the animals were arrested to get food overnight prior to being sacrificed by decapitation. The fresh blood was collected immediately for the number of blood cell analysis. Red blood cells (RBC), white blood cells (WBC), platelet (PLT) counts and hemoglobin (Hb) levels were assessed by using automatic counter system. The spleen, liver and kidney were removed promptly and weighed, and stored at −80 °C for further analysis. The spleen, liver and kidney indexes were calculated.

2.6. Determination of the SOD, CAT and MDA content

The SOD, CAT activities and the MDA content in the liver and kidney homogenates were determined using commercial kits (Nanjing Jiancheng Bioengineering Institute, Nanjing, China). The protein concentration in homogenate was measured by the method of coomassie brilliant blue. The SOD and CAT activities were expressed in U/mg pro, and the content of MDA was expressed in nmol/mg protein (Ye, Chen, Yuan, Ye, & Cai, 2012).

2.7. Assay of splenocyte proliferation

Cell proliferation was determined using MTT-based colorimetric assay. After the mice sacrificed, the spleen collected from the mice under aseptic conditions were grinded into small pieces and passed through sterilized meshes (200 meshes) to obtain a homogeneous cell suspension at the room temperature. The red blood cells were removed by hemolytic red blood cell lysis solution. Recovered splenocytes were washed twice, then resuspended in RMPI-1640 complete medium containing 5% FBS, with cell concentration adjusted to 1×10^6 cell/mL. The cell was seeded in a 96-well plate with or without ConA (5.0 μg/mL). After incubation for 48 h at 37 °C in a humidified 5% CO_2 incubator, the number of cells was determined by MTT assay (Yi et al., 2012).

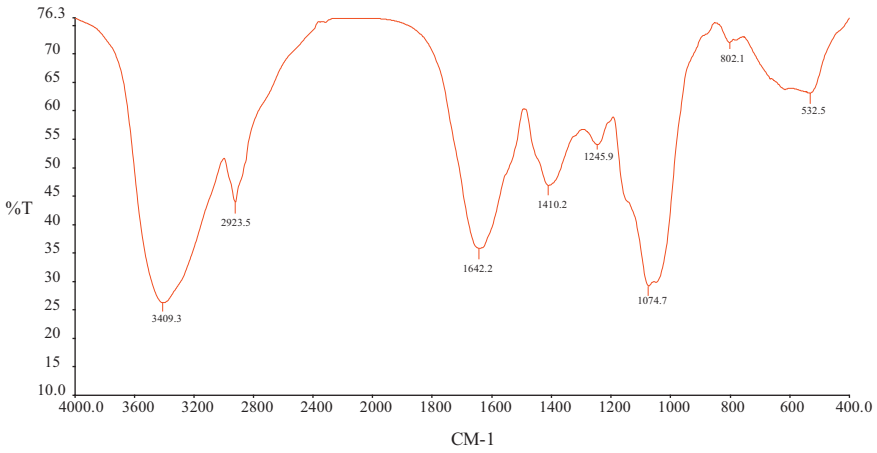

Fig. 1. FT-IR spectra of HSP in the range of 400–4000 cm^{-1}.

2.8. Phagocytosis of monocyte assay

The phagocytosis function of monocyte was determined according to the test of carbon particle clearance with a few modifications. The first 14 days of oral administration and radiation were the same to the Section 2.4. The day after the radiation, 25% (v/v) India ink according to 0.2 mL/kg body weight was injected by a tail intravenous injection. A total of 20 μL of blood was collected through eye orbit after 2 min ($T1$) and 10 min ($T2$), and added to 2 mL 0.1% Na_2CO_3. The absorbance at 600 nm of blood after 2 min ($C1$) and 10 min ($C2$) were measured, and the absorbance of normal control group of blood was set as zero. The mice were sacrificed by decapitation, and then the liver and spleen were weighed. Clearance index (K) and phagocytic index (α) were calculated as follows (Hua et al., 2012):

$$K = \frac{lgC1 - lgC2}{T2 - T1}, \quad \alpha = \sqrt[3]{K} \times \frac{body\ weight}{liver\ weight + spleen\ weight},$$

2.9. Flow cytometric analysis of cell cycle

After the mice sacrificed, the spleen collected from the mice under aseptic conditions were grinded into small pieces and passed through sterilized meshes (200 meshes) to obtain a homogeneous cell suspension at the room temperature. The red blood cells were removed by red blood cell lysis solution for 5 min. Recovered splenocytes were fixed with cold 70% ethanol and stored at 4 °C for at least 24 h, subsequently subjected to PI labeling (PI/RNase Staining Buffer), and the cells were analyzed by flow cytometric (Wei, Wei, Cheng, & Zhang, 2012).

2.10. Endotoxin determination

Endotoxin was measured by commercial kit (Nanjing Jiancheng Bioengineering Institute, Nanjing, China) according to the manufacture's instruction.

2.11. Statistical analysis

All the values were expressed as means ± SD for ten mice in each group. Statistical analysis was performed by one-way analysis of variance (ANOVA) using SPSS (version 16.0). Differences at $p < 0.05$ and $p < 0.01$ were considered statistically significant by Duncan's new multiple-range test.

3. Results and discussion

3.1. Primary structure analysis of HSP

The content of carbohydrate of HSP was 74.33% ± 7.44%. The molecular weight distribution of HSP ranged from 1.19×10^3 to 1.55×10^4 Da by HPGPC. The results of GC-MS showed that HSP was composed of ribose, arabinose, mannose, glucose and galactose in a ratio of 0.65: 0.69: 9.35: 14.24: 5.47. The IR spectrum of HSP was shown in Fig. 1. The high absorbency ranged of 1200–950 cm^{-1} was the characteristic absorption peak of polysaccharide, where the position and intensity of the bands could be identified. The specific intense peaks at 3449 cm^{-1} and 2948 cm^{-1} were attributed to the O—H and C—H stretching vibrations respectively. Characteristically, the bands at 1000–1100 cm^{-1} suggested the existence of pyranose form of the glucosyl residue in HSP. Then, the absorption band at 846.3 cm^{-1} showed the presence of α-linked residues in HSP. The peak at 932 cm^{-1} was due to C—O vibration of 3,6-anhydro-α-L-galactose (Andriamanantoanina, Chambat, & Rinaudo, 2007). The relatively strong absorption peak at around 1634 cm^{-1} revealed the bound water. The absorbance of polysaccharide in the range 1200–950 cm^{-1} was assigned to the C—O—C and C—O—H link band (Li, Wang, Wang, Walid, & Zhang, 2012).

3.2. Effect of HSP on SOD, CAT activities and MDA level in mice

SOD and CAT are the major antioxidant enzymes which block lipid peroxidation and protect the tissue against oxidative damage. MDA, the final product of lipid peroxidation, is regarded as an index of cellular damage and cytotoxicity (Chen et al., 2012a). As showed in Table 1, prominent elevation of MDA level and significant reduction of CAT and SOD in irradiation-induced group were clearly observed in comparison with untreated normal group ($p < 0.05$). However, after the administration of HSP, the MDA content in liver and kidney was significantly reduced, and the levels of SOD and CAT were all increased. Among three HSP doses, at the dosage of 200 mg/kg BW, the SOD and CAT were respectively 288.41 ± 30.21 U/mg protein and 74.05 ± 2.32 U/mg protein in the liver, and respectively 143.06 ± 10.53 U/mg protein and 90.90 ± 6.47 U/mg protein in kidney, which were significantly higher than the contents of SOD and CAT in Model group ($p < 0.05$) and closely to the contents of normal group. However, the MDA level was opposite. Compared with the positive control group Leucogen, oral administration of HSP had the more significant radioprotective effect. The above results showed that HSP could

Table 1
Effect of HSP on SOD, CAT activities and MDA level in kidney and liver of normal and irradiation-induced mice.

Group[a]	SOD (U/mg protein)		CAT (U/mg protein)		MDA (nmol/mg protein)	
	Liver	Kidney	Liver	Kidney	Liver	Kidney
HSP-L	267.09 ± 21.21*	114.61 ± 16.00**	53.19 ± 1.25**,***	65.03 ± 10.31**,***	1.78 ± 0.07**,***	1.78 ± 0.17**,***
HSP-M	267.48 ± 21.23*	131.08 ± 17.46*,***	72.59 ± 3.35*,***	83.35 ± 7.09***	1.56 ± 0.19***	1.38 ± 0.12*,***
HSP-H	288.41 ± 30.21***	143.06 ± 10.53***	74.05 ± 2.32*,***	90.90 ± 6.47***	1.48 ± 0.08***	1.21 ± 0.10***
Leucogen	286.16 ± 19.25***	128.08 ± 13.03*,***	57.21 ± 1.88**,***	74.47 ± 9.76**,***	1.91 ± 0.15**,***	1.48 ± 0.23**,***
Model	257.75 ± 17.64*	97.46 ± 8.16**	46.61 ± 3.21**	41.43 ± 12.17**	2.71 ± 0.24**	2.37 ± 0.10**
Nornal	290.51 ± 23.21	157.21 ± 7.87	78.62 ± 1.24	96.03 ± 9.07	1.35 ± 0.15	0.92 ± 0.30

[a] All values represent the mean ± SD (n = 6).
* Significant difference with Normal group was designated as $p < 0.05$.
** Significant difference with Normal group was designated as $p < 0.01$.
*** Significant difference with Model group was designated as $p < 0.05$.

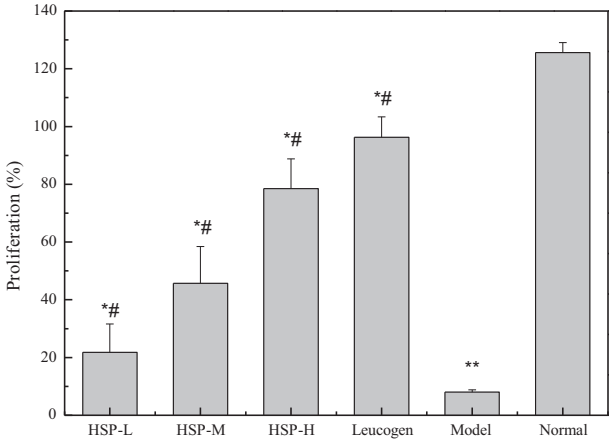

Fig. 2. Effects of HSP on splenocytes proliferation. The data were reported as mean ± SD (n = 6). Significance was determined using the Duncan's new multiple-range test. *Significant difference with Normal group was designated as $p < 0.05$. **Significant difference with Normal group was designated as $p < 0.01$. $^{\#}$Significant difference with Model group was designated as $p < 0.05$.

effectively increase the contents of antioxidant enzymes and lower the level of MDA in the radiation-induced mice. The result was accordance with the study reported by Sui et al. (2013).

3.3. Effect of HSP on splenocyte proliferation

The spleen is the largest immune organ in the vertebrate body, capable of producing a large number of lymphocytes (Xia et al., 2012). The splenocytes proliferation is the most direct indicator of reflecting the state of cellular immunity. The effect of HSP on splenocyte proliferation in the mice was shown in Fig. 2. With the actions of HSP, ConA could significantly stimulate splenocyte proliferation compared with that of model ($p < 0.05$). The 50 and 100 mg/kg HSPs combined with ConA significantly promoted the proliferation of splenocytes. The dose of 200 mg/kg HSP combined with ConA facilitated faster proliferation of splenocytes, but lower than the effect of the positive control. The splenocyte proliferation response was related to immunity improvement of T-lymphocytes or B-lymphocytes (Marciani et al., 2000). The results indicated that HSP possessed a definite and clear synergistic action on splenocyte proliferation after combining with ConA.

3.4. Effects on blood cell counts and hemoglobin concentration

Ionizing radiation can cause the medulla hemopoietic function suppressed and the number of WBC decreased in blood, especially irradiation with a high dose could lay significant inhibition on building blood in medulla and extramedulla (Chen et al., 2012b). As shown in Table 2, the haematologic parameters (including WBC, RBC and PLT counts, and the concentration of HGB) in model group decreased significantly compared with normal group ($p < 0.05$). However, with the administration of HSP, the counts of WBC, RBC and PLT, and the concentration of HGB were all increased in a dose-dependent manner. Among three doses (50, 100 and 200 mg/kg BW), the high dose of HSP possessed the most significant protective effect ($p < 0.05$) against the damage of radiation except the brilliant protective action of RBC was the medium dose. According to the statistical analysis of the protective effect of HSP to RBC in blood was not significant, and lower than that of the Positive control group (Leucogen). The results indicated that HSP could effectively protect the number of the blood WBC decrease and the function of hematopoietic decline which caused by irradiation.

3.5. Effect of HSP on phagocytosis of monocyte in mice

Monocyte is the most important phagocyte and plays an important role immune response. The phagocytosis of monocytes was reflected by the test of carbon clearance (Yang, Guo, Zhang, & Wu, 2007). Table 3 showed that the effect of HSP on the phagocytosis in mice. In comparison with the Normal group, the phagocytic index (PI) of Model group was much lower ($p < 0.01$). After the administration of HSP, the phagocytic indexes were all increased in a

Table 2
Effect of HSP on blood cell counts and hemoglobin concentration in the normal and irradiation-induced mice.

Group[a]	WBC (10^9/L)	RBC (10^{12}/L)	PLT (10^{11}/L)	HGB (G/L)
HSP-L	1.72 ± 0.52**	7.84 ± 0.98	0.82 ± 0.72**	127.36 ± 9.56**
HSP-M	2.24 ± 0.45**	9.28 ± 2.04	4.59 ± 0.89**,***	160.54 ± 21.32***
HSP-H	3.12 ± 1.01*****	8.23 ± 1.20	8.45 ± 2.01***	166.21 ± 14.24***
Leucogen	4.61 ± 0.85*,***	9.78 ± 1.25***	4.77 ± 1.01**,***	174.01 ± 12.22***
Model	1.70 ± 0.21**	6.93 ± 0.32	0.58 ± 0.11**	120.00 ± 14.23**
Normal	6.04 ± 1.33	9.27 ± 0.78	7.20 ± 1.34	165.46 ± 9.36

[a] All values represent the mean ± SD (n = 6).
* Significant difference with Normal group was designated as $p < 0.05$.
** Significant difference with Normal group was designated as $p < 0.01$.
*** Significant difference with Model group was designated as $p < 0.05$.

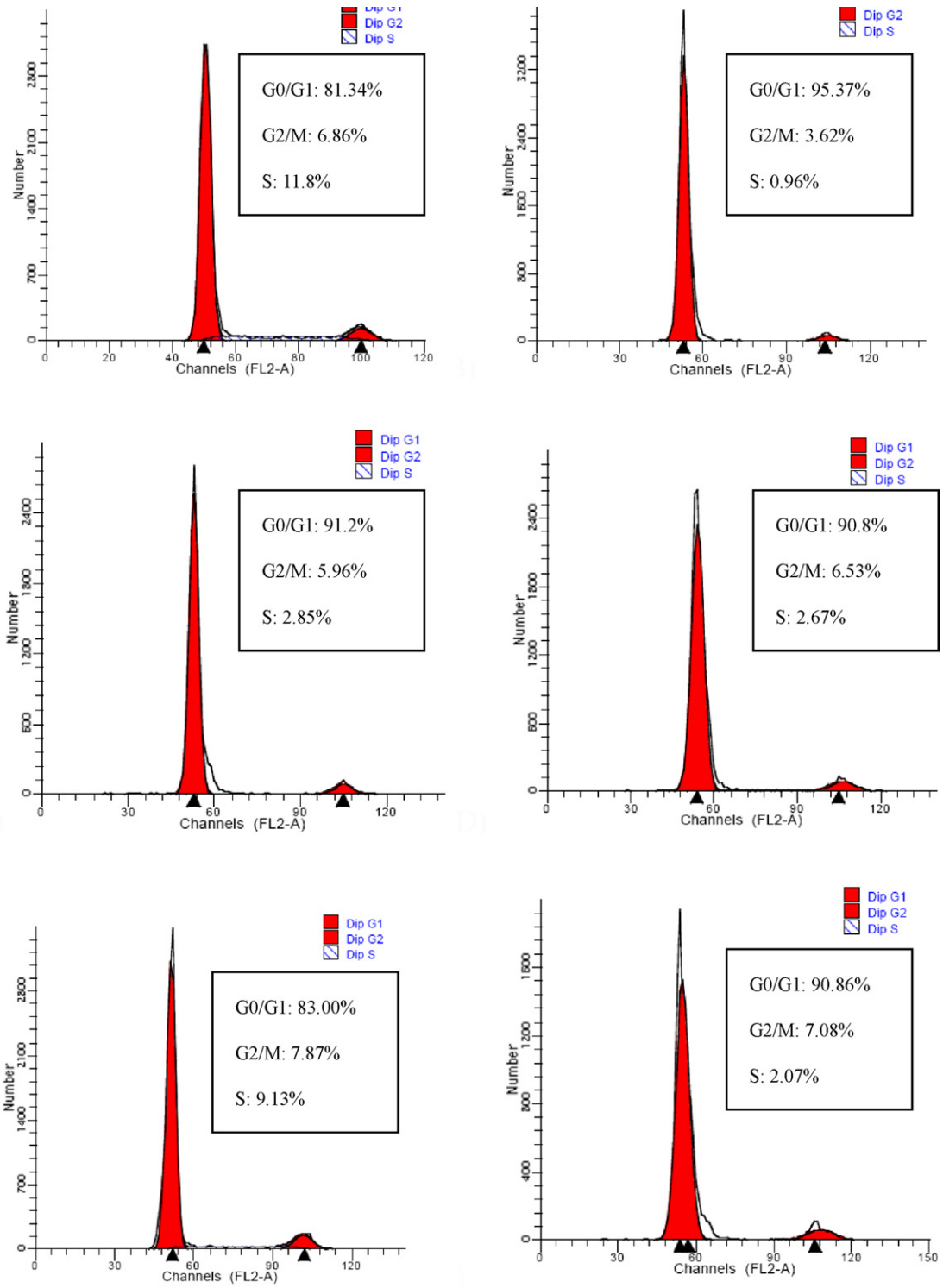

Fig. 3. Cell-cycle analysis of splenocytes treated with HSP. (A) Normal group; (B) Model group; (C) Low concentration of HSP group; (D) Medium concentration of HSP group; (E) High concentration of HSP group; (F) Positive control group (Leucogen).

dose-dependent manner. Both of indexes in high dose (200 mg/kg BW) group and medium dose (150 mg/kg BW) group were higher that that in Positive control group. No significant difference was found between low dose group and Model group ($p > 0.05$). The above result revealed that HSP could significantly improve the phagocytosis of monocyte in mice.

The liver and kidney are important organs and spleen is the largest immune organ in the body. Their weights could be well reflected the damages of body induced by irradiation. Radioprotectors could increase the weight of these organs (Chen et al., 2012c). As shown in Table 3, liver index and spleen index of Model group mice were both much lower than those of Normal group mice ($p < 0.01$), respectively. The kidney indexes of all groups were no significant difference ($p > 0.05$). After the treatment with HSP, the liver index and spleen index were all increased in a dose-dependent manner, especially the spleen index. At the dose of 200 mg/kg BW, all the organ indexes were higher than the indexes of the Positive control group, and much closer to the indexes of the

Table 3
Effects of HSP on the phagocytosis of monocyte and organ indexes in mice.

Group[a]	Phagocytic index	Liver index	Spleen index	Kidney index
HSP-L	5.41 ± 0.21**	4.34 ± 0.08**	0.19 ± 0.01**	1.27 ± 0.02
HSP-M	6.28 ± 0.39*,***	5.17 ± 0.66**	0.25 ± 0.05**	1.28 ± 0.12
HSP-H	6.98 ± 0.41***	6.52 ± 0.48***	0.45 ± 0.02***	1.29 ± 0.16
Leucogen	5.89 ± 0.37**,***	5.16 ± 0.65**	0.21 ± 0.03**	1.33 ± 0.34
Model	5.01 ± 0.29**	4.60 ± 0.61**	0.18 ± 0.03**	1.26 ± 0.02
Normal	7.11 ± 0.19	6.94 ± 0.08	0.36 ± 0.09	1.38 ± 0.09

[a] All values represent the mean ± SD ($n = 6$).
* Significant difference with Normal group was designated as $p < 0.05$.
** Significant difference with Normal group was designated as $p < 0.01$.
*** Significant difference with Model group was designated as $p < 0.05$.

Normal group. The results indicated that HSP could improve the organ indexes against the effect of the radiation.

3.6. Cell-cycle arrest induced by radiation in mice splenocyte

Polysaccharide could protect the cells against the damage induced by irradiation. Fig. 3 showed the effect of HSP on the cell-cycle phase (G0/G1, S, and G2/M) distribution of splenocytes by flow cytometry with PI staining. In comparison with the Normal group (81.34%), more splenocytes of Model group were arrested in G0/G1 phase (95.37%). After treatment with different concentrations of HSP, the cells in G0/G1 phase were decreased in a dose-dependent manner and changed into the S phase. At the concentration of 200 mg/kg BW, the cells in G0/G1 and S phases were 83.00% and 9.13%, respectively. HSP did not induce the significant change in G2/M phase at the tested concentrations. The results suggested that HSP could protect the splenocytes against the damage caused by radiation through inhibiting more cells arrest into G0/G1 phase, and promote the splenocyte proliferation.

3.7. Endotoxin content

Lipopolysaccharides (LPS) possess several immunomodulation activities, such as activation of immune cell. Therefore, LPS contamination could result to false positive results of biological experiments. We have analyzed the endotoxin content in HSP and the result suggested that HSP contain no endotoxin.

4. Conclusion

In the present study, we investigated the antioxidant, immunomodulatory and radioprotective activities of the polysaccharides from *H. serotina* in vivo. The results showed that HSP could significantly increase the effects of SOD and CAT, lower the MDA level in mice which were exposed to the ^{60}Co-radiation compared to the irradiated, non-treated controls. Furthermore, HSP could improve the immunomodulatory activities, including proliferation of splenocytes, the amount of WBC of blood and phagocytosis of monocyte in mice. Through the cell-cycle assay of splenocytes, HSP significantly inhibit the cells arrest into G0/G1 phase and effectively protect the cells away from irradiation-induced damage. The biological activities of HSP may correlate to their specific structures. We have reported that the primary structure of the crude polysaccharide (HSP), so further research is needed to analyze the complete structure, mechanism of anti-radiation activity and the relationship between the function and structure. It is definite that the HSP can be exploited because of the significant biological activities.

Acknowledgement

The authors thank Prof Lan-Wei Zhang and Prof Ying Ma from the School of Food Science and Engineering, Harbin Institute of Technology, for helpful suggestions and assistance.

References

Andriamanantoanina, H., Chambat, G., & Rinaudo, M. (2007). Fractionation of extracted Madagascan Gracilaria corticata polysaccharides: Structure and properties. *Carbohydrate Polymers*, *68*, 77–88.
Bansal, P., Paul, P., Kunwar, A., Jayakumar, S., Nayak, P. G., Priyadarsini, K. I., et al. (2012). Radioprotection by quercetin-3-O-rutinnoside a flavonoid glycoside – A cellular and mechanistic approach. *Journal of Functional Foods*, *4*, 924–932.
Chen, Q., Zhang, S. Z., Ying, H. Z., Dai, X. Y., Li, X. X., Yu, C. H., et al. (2012). Chemical characterization and immunostimulatory effects of a polysaccharide from *Polygoni Multiflori Radix Praeparata* in mice. *Carbohydrate Polymers*, *88*, 1476–1482.
Chen, X. M., Nie, W. J., Yu, G. Q., Li, Y. L., Hu, Y. S., Lu, J. X., et al. (2012). Antitumor and immunomodulatory activity of polysaccharides from *Sargassum fusiforme*. *Food and Chemical Toxicology*, *50*, 695–700.
Chen, Y., Tang, J. B., Wang, X. K., Sun, F. X., & Liang, S. J. (2012). An immunostimulatory polysaccharide (SCP-IIa) from the fruit of *Schisandra chinensis* (Turcz.) Baill. *International Journal of Biological Macromolecules*, *50*, 844–848.
Cheng, H. R., Feng, S. L., Jia, X. J., Li, Q. Q., Zhou, Y. H., & Ding, C. B. (2013). Structural characterization and antioxidant activities of polysaccharides extracted from *Epimedium acuminatum*. *Carbohydrate Polymers*, *92*, 63–68.
Hsu, W. K., Hsu, T. H., Lin, F. Y., Cheng, Y. K., & Yang, J. P. W. (2013). Separation, purification and α-glucosidase inhibition of polysaccharides from *Coriolus versicolor* LH1 mycelia. *Carbohydrate Polymers*, *92*, 297–306.
Hua, Y. L., Gao, Q., Wen, L. R., Yang, B., Tang, J., You, L. J., et al. (2012). Structural characterization of acid- and alkali-soluble polysaccharides in the fruiting body of *Dictyophora indusiata* and their immunomodulatory activities. *Food Chemistry*, *132*, 739–743.
Lata, M., Prasad, J., Singh, S., Kumar, R., Singh, L., Chaudhary, P., et al. (2009). Whole body protection against lethal ionizing radiation in mice by REC-2001: A semi-purified fraction of *Podophyllum hexandrum*. *Phytomedicine*, *16*, 47–55.
Li, X. Y., Wang, Z. Y., Wang, L., Walid, E., & Zhang, H. (2012). Ultrasonic-assisted extraction of polysaccharides from *Hohenbuehelia serotina* by response surface methodology. *International Journal of Biological Macromolecules*, *51*, 523–530.
Liu, J. C., Sun, Y. X., Yu, C. L., & Liu, L. (2012). Chemical structure of one low molecular weight and water-soluble polysaccharide (EFP-W1) from the roots of *Euphorbia fischeriana*. *Carbohydrate Polymers*, *87*, 1236–1240.
Marciani, D. J., Press, J. B., Reynolds, R. C., Pathak, A. K., Pathak, V., Gundy, L. E., et al. (2000). Development of semisynthetic triterpenoid saponin derivatives with immune stimulating activity. *Vaccine*, *18*, 3141–3151.
Park, E., Hwang, I., Song, J. Y., & Jee, Y. (2011). Acidic polysaccharide of *Panax ginseng* as a defense against small intestinal damage by whole-body gama irradiation of mice. *Acta Histochemica*, *113*, 19–23.
Patra, P., Sen, I. K., Bhanja, S. K., Nandi, A. K., Samanta, S., Das, D., et al. (2013). Pectic polysaccharide from immature onion stick (*Allium cepa*): Structural and immunological investigation. *Carbohydrate Polymers*, *92*, 345–352.
Sui, Z. F., Li, L., Gu, T. M., Zhao, Z. L., Liu, C., Shi, C. F., et al. (2013). Optimum conditions for *Radix Rehmanniae* polysaccharides by RSM and its antixoidant and immunity activity in UVB mice. *Carbohydrate Polymers*, *92*, 283–288.
Sun, Y., Sun, T. W., Wang, F., Zhang, J., Li, C., Chen, X. N., et al. (2013). A polysaccharide from the fungi of Huaier exhibits anti-tumor potential and immunomodulatory effects. *Carbohydrate Polymers*, *92*, 577–582.
Thotala, D., Chetyrkin, S., Hudson, B., Hallahan, D., Voziyan, P., & Yazlovitskaya, E. (2009). Pyridoxamine protects intestinal epithelium from ionizing radiation-induced apoptosis. *Free Radical Biology and Medicine*, *47*, 779–785.
Wang, J. G., Wang, Y. T., Liu, X. B., Yuan, Y. H., & Yue, T. L. (2013). Free radical scavenging and immubomodulatory activities of *Ganoderma lucidum* polysaccharides derivatives. *Carbohydrate Polymers*, *91*, 33–38.
Wang, Y. F., Mao, F. F., & Wei, X. L. (2012). Characterization and antioxidant activities of polysaccharides from leaves flowers and seeds of green tea. *Carbohydrate Polymers*, *88*, 146–153.
Wei, D. F., Wei, Y. X., Cheng, W. D., & Zhang, L. F. (2012). Sulfated modification characterization and antitumor activities of *Radix hedysari* polysaccharide. *International Journal of Biological Macromolecules*, *51*, 471–476.
Xia, L. J., Liu, X. F., Guo, H. Y., Zhang, H., Zhu, J., & Ren, F. Z. (2012). Partial characterization and immunomodulatory activity of polysaccharides from the stem of *Dendrobium officinale* (Tiepishihu) in vitro. *Journal of Functional Foods*, *4*, 294–301.

Yang, W. J., Pei, F., Shi, Y., Zhao, L. Y., Fang, Y., & Hu, Q. H. (2012). Purification characterization and anti-proliferation activity of polysaccharides from *Flammulina velutipes*. *Carbohydrate Polymers*, *88*, 474–480.

Yang, X. P., Guo, D. Y., Zhang, J. M., & Wu, M. C. (2007). Characterization and antitumor activity of pollen polysaccharide. *International Immunopharmacology*, *7*, 427–434.

Ye, M., Chen, W. X., Yuan, R. Y., Ye, Y. W., & Cai, J. M. (2012). Structural characterization and anti-aging activity of extracellular polysaccharide from a strain of *Lachnum* sp. *Food Chemistry*, *132*, 338–343.

Yi, Y., Zhang, M. W., Liao, S. T., Zhang, R. F., Deng, Y. Y., Wei, Z. C., et al. (2012). Structural features and immunomodulatory activities of polysaccharides of longan pulp. *Carbohydrate Polymers*, *87*, 636–643.

Ying, Z., Han, X. X., & Li, J. R. (2011). Ultrasound-assisted extraction of polysaccharides from mulberry leaves. *Food Chemistry*, *127*, 1273–1279.

Yu, J., Piao, B. K., Pei, Y. X., Qi, X., & Hua, B. J. (2010). Protective effects of tetrahydropalmatine against γ-radiation induced damage to human endothelial cells. *Life Science*, *87*, 55–63.

Zhao, L., Wang, Y., Shen, H. L., Shen, X. D., Nie, Y., Wang, Y., et al. (2012). Structual characterization and radioprotection of bone marrow hematopoiesis of two novel polysaccharides from the root of *Angelica sinensis* (Oliv.) Diels. *Fitoterapia*, *83*, 1712–1720.

Zou, Y. F., Chen, X. F., Yang, W. Y., & Liu, S. (2011). Response surface methodology for optimization of the ultrasonic extraction of polysaccharides from *Codonopsis pilosula* Nannf Var. *modesta* L.T. Shen. *Carbohydrate Polymers*, *84*, 503–508.